Contrast

OVERVIEW

We have seen that the SNR (signal-to-noise ratio) determines the effectiveness of an imaging experiment. However, even the highest SNR does not guarantee the usefulness of an image. An important aim of imaging for diagnostic purposes is to be able to distinguish between diseased and neighboring normal tissues. If the imaging method used does not have a signal-manipulating mechanism which produces different signals for the diseased and normal tissues, then distinguishing the two tissues is not possible. MRI is blessed with an abundance of contrast-producing mechanisms, as the signal is dependent on a wide variety of tissue parameters. The problem of distinguishing a given (diseased) structure from surrounding (normal) tissue in the presence of added white noise falls under the broad category of the "signal-detection" problem, and requires an understanding of the importance of the contrast-to-noise ratio (CNR).

The common way to look at this problem is to examine the absolute signal difference between the two tissues of interest. If these tissues are labeled A and B, their signal difference is defined as the "contrast":

$$C_{AB} \equiv S_A - S_B \qquad \textbf{(B6.3.1)}$$

where S_A and S_B are the voxel signals from tissues A and B, respectively. Although the inherent contrast may be large enough to detect a change, if the noise is too large, the signal difference would not be visible to the eye or to a simple signal-difference threshold algorithm. The more appropriate measure is the ratio of the contrast to the noise standard deviation, known as the contrast-to-noise ratio (CNR):

$$\mathrm{CNR}_{AB} \equiv \frac{C_{AB}}{\sigma_0} = \left|\frac{S_A - S_B}{\sigma_0}\right| = \left|\mathrm{SNR}_A - \mathrm{SNR}_B\right| \qquad \textbf{(B6.3.2)}$$

The utility of this definition is best illustrated with a simple discussion of statistics. For Gaussian-distributed white noise, the probability that two tissues are different if CNR_{AB} equals $2\sqrt{2}$ is 95%, and, if CNR_{AB} equals $3\sqrt{2}$, it is 99%. Ideally, we would like to design the MR experiment to have sufficient spatial resolution to resolve the two tissues of interest (such as gray matter and white matter) and to have a high enough CNR that they can be distinguished from each other. It is important to mention that Equation B6.3.2 assumes that the signal-to-noise ratios of tissues A and B satisfy the minimum SNR requirement (varying between 3 to 5) for a confident object detection as described by the *Rose Criterion* (Rose, 1985). An example of how the object detection for a given CNR is affected by the object size and SNR is shown in Figure B6.3.2.

As mentioned earlier, MRI has the flexibility to manipulate the tissue signal in many ways, leading to numerous contrast mechanisms. The flexibility arises from the MR signal dependence on many imaging and tissue parameters. The most basic contrast-generating mechanisms result from spin density, T_1 and T_2, differences between tissues. Other mechanisms are based upon flow, magnetic susceptibility differences, magnetization transfer contrast, tissue saturation methods, contrast enhancing agents, and diffusion. With these basic contrast mechanisms, the MR image is weighted toward one of the parameters.

Contributed by Azim Celik and Weili Lin

Current Protocols in Magnetic Resonance Imaging (2002) B6.3.1-B6.3.14

The general signal for a gradient-echo experiment contains a combination of dependence on all three basic MR properties via:

$$S = \rho_0 (1 - e^{-T_R / T_1}) e^{-T_E / T_2^*} \quad \textbf{(B6.3.3)}$$

Spin density weighting can be achieved by minimizing the tissue contrast on T_1 and T_2^*. The choice of a long T_R ($>> T_1$) allows enough time for the signal to recover, and, therefore, minimizes the signal dependence on T_1. Likewise, for a short T_E ($<< T_2^*$), the effect of relaxation time on the signal will be minimal. Therefore, a long T_R and short T_E produce spin density weighting, which enhances the spin density contrast between two tissues. On the other hand, intermediate T_R ($\leq T_1$) and short T_E ($<<T_2^*$) produce T_1-weighting, while a long T_R ($>>T_1$) and long T_E ($\leq T_2^*$) produce T_2^*-weighting. It is necessary to keep in mind that both T_1-weighted and T_2^*-weighted (or T_2 for spin echo imaging) images are weighted by spin density as well.

Spin density weighting is especially valuable for the estimation of water content in one tissue relative to another tissue. T_1-weighting is commonly used to obtain enhanced soft tissue contrast. The T_1 contrast as a function of repeat time is shown in Figure B6.3.4 for different combinations of CSF (cerebrospinal fluid), GM (gray matter), WM (white matter), and lesion-containing tissue. Evidently, the contrast between different tissues can be maximized with the appropriate choice of T_R. Finally, T_2- or T_2^*-weighted contrast is more suitable for the delineation of diseased structures characterized by an elevated T_2. The T_2 contrast between different soft tissues and between GM and lesion is illustrated in Figure B6.3.5 as a function of echo time. An example of spin-density weighted, T_1-weighted, and T_2-weighted MR images is shown in Figure B6.3.6 using a conventional spin echo sequence. Notice the superior contrast in the T_1-weighted image between different tissue types.

In the subsequent sections of this unit, a brief introduction to object visibility and Rose criterion will be followed by a discussion on the three basic forms of contrast mechanisms: spin density weighted contrast, T_1-weighted contrast, and T_2 (or T_2^*)-weighted contrast.

TECHNICAL DISCUSSION

Object Visibility and the Rose Criterion

The final interpretation of data comes from the physician evaluating the images by eye. Our visual system is an intelligent step in the viewing process and tends to locally average parts of an image. Here, we consider what effect this has on the visibility of an object.

If multiple independent signal measurements N_{acq} are performed, an average of these signal measurements implies that the effective noise standard deviation becomes:

$$\sigma_{eff} = \frac{\sigma_0}{\sqrt{N_{acq}}} \quad \textbf{(B6.3.4)}$$

In an image where tissue A occupies n_{voxel} voxels, each of which has signal S_A with independent additive white noise of standard deviation σ_0, a similar voxel-averaging scenario can be incorporated into the detection criterion (with N_{acq} replaced by n_{voxel}) via a new measure referred to as the "object visibility" or:

$$\nu_{AB} \equiv \frac{C_{AB}}{\sigma_{eff}} = \frac{C_{AB}}{\sigma_0}\sqrt{n_{voxel}} = CNR_{AB}\sqrt{n_{voxel}} \quad \textbf{(B6.3.5)}$$

where C_{AB} is defined in Equation B6.3.1. Again, the noise in each voxel of the image, σ_0, is assumed to be the same for both tissues.

The Rose criterion

The visibility threshold can be determined empirically. Based on experiments with human observers detecting circular objects shown on a television screen, Rose found that random fluctuations in the photon flux forming the object confused the observer, and a minimum "SNR" was required for confident object detection. Depending on the observer's expertise and what is being observed, a detection SNR threshold varying between 3 and 5 was found to be required for object recognition. This requirement is known as the "Rose Criterion" in the diagnostic imaging literature.

A visibility threshold of ~4 can be reinterpreted for the tissue discrimination problem as follows: a Gaussian model for the additive white noise is found to be a rather good approximation for the thermal noise. With this assumption made, the image signals from tissues A and B can be modeled by two Gaussian distributions centered at S_A and S_B, respectively, with the same standard deviation, σ_0. Now, if $S_A - S_B = 4\sigma_0$, as it would be for single-voxel tissues A and B, the two Gaussian distributions are separated by $4\sigma_0$ (see Figure B6.3.1). Since a distance $2\sigma_0$ to one side of the mean covers ~97.5% of the area under a Gaussian, it is reasonable to expect the human observer to choose a threshold which is $2\sigma_0$ away from either S_A or S_B. Then, the probability of the observer incorrectly classifying a voxel as belonging to one or the other tissue is 0.025, i.e., the chance of this occurring is 1-in-40. That is, the probability of detection of the tissue is very high: for a multi-voxel object when ν equals 4, only 1 in 40 voxels in the object will be classified incorrectly by the observer as a background voxel, and vice-versa; for a single-voxel object, there is only a 1-in-40 chance of not detecting it. This description is essentially a rule of thumb, as the perception of the object is likely to be much more complicated.

The effect of object size, σ_0 and contrast level on object visibility can be demonstrated visually to be determined by the quantity ν, as defined in Equation B6.3.5, by observing the images in Figure B6.3.2. The model image with no noise added is shown in Figure B6.3.2A. The simulated objects are disk-like objects of linearly decreasing radius (5-voxel radius to 1-voxel radius) going from top to bottom and linearly increasing signal values going from left to right (doubling from column 1 to column 5; actual values can be

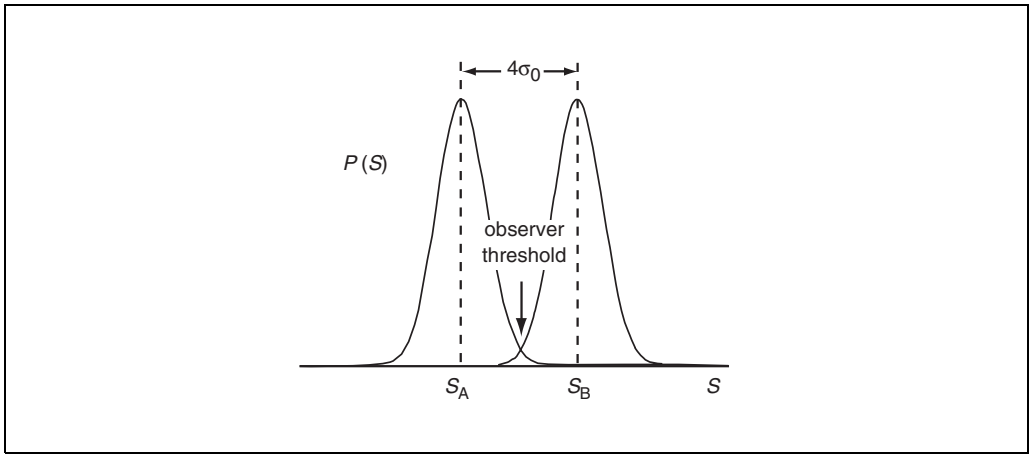

Figure B6.3.1 Image signal distribution of two tissues, A and B, with added Gaussian distributed white noise. When $|S_A - S_B|$ equals $4\sigma_0$, the probability of an error in the detection of tissue *A* is ~0.025 when a threshold of $2\sigma_0$ is used. Likewise, the probability of misclassifying a noise point as an object is also 0.025. If this were the criteria by which our visual system worked, then we would recognize objects when visibility was 4.

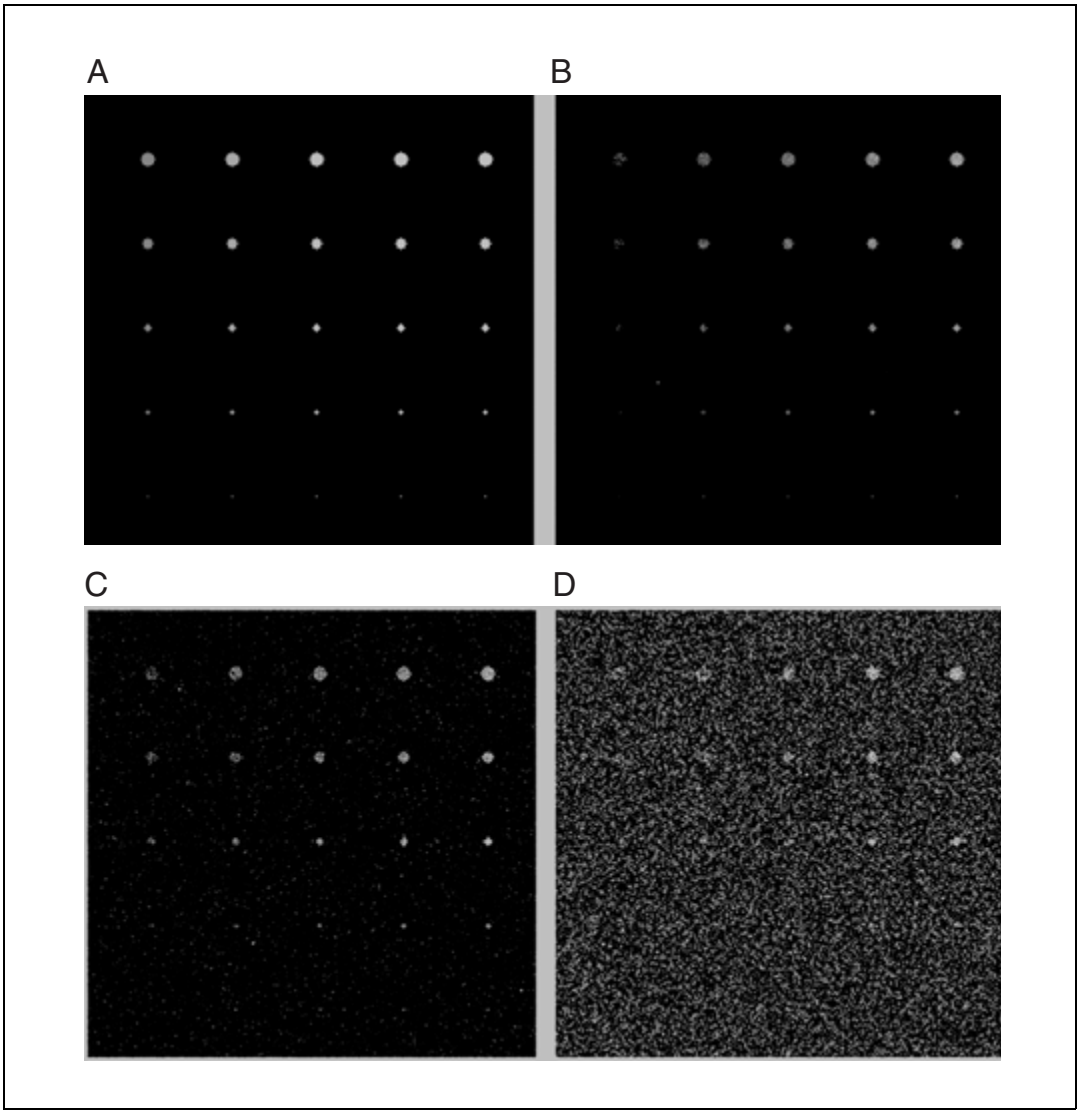

Figure B6.3.2 Images designed to show how visibility of large and small objects changes as a function of CNR, and how their detection for a given CNR depends on the object size. For the cases shown, CNR is the same as SNR since each feature is being compared to the background noise. (**A**) Model of circles with no background noise (SNR = ∞); (**B**) SNR = 4; (**C**) SNR = 2; and (**D**) SNR = 1. The SNR values quoted for these images are measured relative to the objects with lowest signal (column 1). As mentioned in the text, SNR doubles for the rightmost column in comparison with the leftmost column in each image.

computed from SNR values quoted in the caption for Fig. B6.3.2) imaged in a zero-signal background. The model image is assumed to be all real, whereas the noise is assumed to have uncorrelated and equal expected power in both the real and imaginary image channels. The noisy images were created by adding the real channel noise to the model and taking the magnitude of the two image channels after this addition. As seen in Figure B6.3.2, the smaller disks become indistinguishable from noise at the lower SNR levels while the larger disks are detectable even at degraded SNR levels. Also, the higher the true contrast of the object, the higher the SNR degradation must be before such an object becomes undetectable. It is easy to note that at a given SNR level (images at different SNR levels are shown in Fig. B6.3.2B to B6.3.2D), an imaginary diagonal line can be drawn separating the barely detectable objects from the undetectable objects and the clearly detectable objects. It is found that the objects along such a diagonal line have a constant value of the product of the signal with the square root of the number of voxels

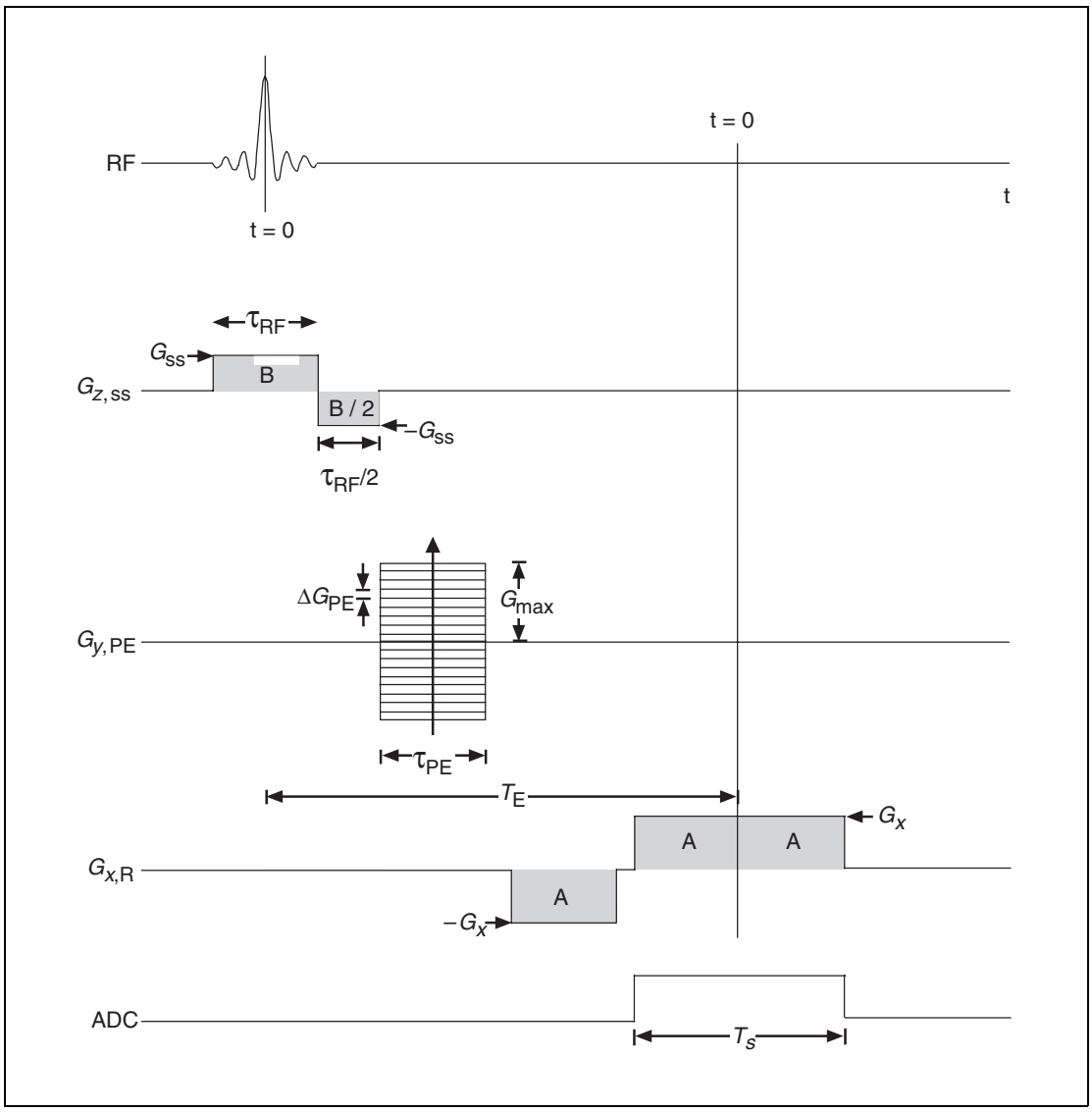

Figure B6.3.3 A 2-D gradient echo sequence diagram.

occupied by the object. This empirically demonstrates that the threshold of visibility is determined by the quantity ν defined in Equation B6.3.5.

Contrast Mechanisms in MRI and Contrast Maximization

A 90° gradient echo experiment is used as an example of how to obtain different forms of contrast. These results are identical to those that would be found for a 90° spin echo experiment under the assumption that $T_E << T_R$ and T_2 is replaced by T_2^*. Different expressions and relations must be derived for other imaging techniques.

Although each type of contrast is designed to enhance differences in one of the specified parameters (ρ_0, T_1 or T_2), the signal is a function of all three variables, and each must be kept in mind when determining overall image contrast. As an illustrative example, the contrast between tissues A and B for a 90° flip angle gradient echo experiment (see Fig. B6.3.3) is:

$$C_{AB} = S_A(T_E) - S_B(T_E) = \rho_{0,A}\left(1 - e^{-T_R/T_{1,A}}\right)e^{-T_E/T^*_{2,A}} - \rho_{0,B}\left(1 - e^{-T_R/T_{1,B}}\right)e^{-T_E/T^*_{2,B}} \quad \textbf{(B6.3.6)}$$

Note that the signal is assumed to be determined by the tissue signal solution from the Bloch equation at the echo time T_E. One must remember that this time corresponds to the $k = 0$ sample in the read direction. C_{AB} can then be maximized with respect to either T_R or T_E.

Spin density weighting

In order to get contrast based primarily on ρ_0, the T_1 and T_2^* dependence of the gradient echo tissue signals must be minimized. When the argument of an exponential is small, an appropriate approximation to e^{-x} is $(1 - x)$ which is better written as $1 - \mathcal{O}(x)$. If the exponent is large and negative, e^{-x} can be approximated by zero. It is seen that in order to maintain adequate signal and get contrast based primarily upon spin density, appropriate choices of T_E and T_R would be:

$$T_E \ll T^*_{2_{A,B}} \Rightarrow e^{-T_E/T_2^*} \to 1 \quad \textbf{(B6.3.7)}$$

$$T_R \gg T_{1_{A,B}} \Rightarrow e^{-T_R/T_1} \to 0 \quad \textbf{(B6.3.8)}$$

and Equation B6.3.6 for the contrast between tissues becomes:

$$C_{AB} = (\rho_{0,A} - \rho_{0,B}) - \rho_{0,A}\left(e^{-T_R/T_{1,A}} + \frac{T_E}{T^*_{2,A}}\right) + \rho_{0,B}\left(e^{-T_R/T_{1,B}} + \frac{T_E}{T^*_{2,B}}\right) + \text{higher order and cross terms} \simeq \rho_{0,A} - \rho_{0,B} \quad \textbf{(B6.3.9)}$$

In this approximation, the contrast does not depend upon T_R or T_E, and need not be extremized relative to either T_R or T_E. This gives a general rule for spin-density weighting: keep T_R much longer than the longest T_1 component; keep T_E much shorter than the shortest of T_2^* component. The gradient echo image contrast is then primarily determined by spin-density differences. Similar rules will be formed for T_1-weighting and T_2^*-weighting based on the practical limits imposed on T_E and T_R. These limits are summarized in Table B6.3.1. The actual error in this approximation of spin density weighting of the signal depends on the coefficients for T_E/T_2^* and T_R/T_1, the former vanishing only linearly in T_E/T_2^*. In practice, this means that most imaging experiments still have an error of a few percent, even if T_E is as low as a few milliseconds, since some typical T_2^* values are on the order of tens of milliseconds.

One important application of spin density imaging is to estimate the water content of one tissue relative to another tissue from their contrast differences for a spin-density-weighted sequence. For example, consider a gradient echo experiment with $T_R = 5$ sec, $T_E = 5$ msec

Table B6.3.1 General Set of Rules for Generating Tissue Contrast

Type of contrast	T_R	T_E
Spin density	As long as possible	As short as possible
T_1-weighted	On the order of the T_1 values	As short as possible
T_2-weighted	As long as possible	On the order of the T_2 values

and a $\pi/2$ pulse. Assume that ρ_0, T_1, and T_2 for two adjacent tissues are 1.0, 2 sec, 20 msec for tissue A and 0.8, 1 sec, and 50 msec for tissue B. Then, the estimated spin density for these two tissues using Equation B6.3.9 would be 0.715 and 0.723 for tissues A and B, respectively. Clearly, the first-order effects of nonzero T_E and finite T_R must be included to estimate spin density properly.

Practically, the minimum T_E is limited by the available gradient strength. In fact, this limitation made the imaging of rigid solids impossible for many years because their T_2^* values are on the order of a few hundred microseconds to several milliseconds, and no hardware was available which could form an echo before the signal was gone. However, with modern hardware and modern imaging techniques, solids imaging is now viable. T_E is also limited by the highest acceptable readout bandwidth/voxel (or lowest possible T_s) for SNR, and object-visibility considerations. The maximum value of T_R, on the other hand, is constrained by imaging-time and imaging-efficiency considerations. Therefore, true spin density weighting using a 90° gradient echo sequence is practically achievable only for tissues with long enough T_2^* values and short enough T_1 values, which allow T_E and T_R choices that satisfy the constraints imposed by the gradient strength limitation, the SNR, and imaging time. Good spin-density-weighted contrast is available for most purposes without requiring a zero T_E or infinite T_R.

So far, we have focused on gradient echo sequence but have ignored spin-echo sequence. How does the contrast manifest itself in a spin-echo experiment? Before we address this question, let us look at the contrast for a repeated spin-echo experiment:

$$\begin{aligned} C_{AB} = S_A - S_B &= \rho_{0,A}(1 - 2e^{-(T_R-\tau)/T_{1,A}} + e^{-T_R/T_{1,A}})e^{-T_E/T_{2,A}} \\ &\quad - \rho_{0,B}(1 - 2e^{-(T_R-\tau)/T_{1,B}} + e^{-T_R/T_{1,B}})e^{-T_E/T_{2,B}} \\ &\simeq \rho_{0,A}(1 - e^{-T_R/T_{1,A}})e^{-T_E/T_{2,A}} - \rho_{0,B}(1 - e^{-T_R/T_{1,B}})e^{-T_E/T_{2,B}} \end{aligned} \qquad \textbf{(B6.3.10)}$$

$$\text{for } T_R \gg T_E = 2\tau \qquad \textbf{(B6.3.11)}$$

where τ is the time between the 90° and 180° RF pulses.

Basically, the only difference between the gradient and spin-echo experiments is the T_2^* or T_2 dependence. Therefore, for a tissue with long enough T_2^*, good spin density weighting can be obtained using either spin-echo or gradient-echo sequences. However, for a tissue with short T_2^* or in the presence of large field inhomogeneties, the spin-echo sequence has a distinct advantage over gradient-echo sequences in producing spin-density-weighted images due to its dependence on T_2 rather than T_2^*.

T_1-weighting

Normal soft tissue T_1 values are quite different from one another. For this reason, T_1-weighted contrast offers a very powerful method for delineation of different tissues.

For T_1-weighting, T_2^* effects have to be minimized. Using the gradient echo example as before, the choice of a very short T_E again reduces any T_2^* (or T_2) contrast, i.e., T_E is chosen such that:

$$T_E \ll T^*_{2_{A,B}} \Rightarrow e^{-T_E/T_2^*} \rightarrow 1 \qquad \textbf{(B6.3.12)}$$

and the expression for the contrast is now:

$$\begin{aligned} C_{AB} &= S_A(T_E) - S_B(T_E) \\ &\simeq \rho_{0,A}\left(1 - e^{-T_R/T_{1,A}}\right) - \rho_{0,B}\left(1 - e^{-T_R/T_{1,B}}\right) \quad T_E \ll T^*_{2_{A,B}} \\ &= (\rho_{0,A} - \rho_{0,B}) - \left(\rho_{0,A} e^{-T_R/T_{1,A}} - \rho_{0,B} e^{-T_R/T_{1,B}}\right) \end{aligned} \qquad \textbf{(B6.3.13)}$$

Since there is no transverse relaxation dependence in the above expression, this expression is equally valid for a spin echo sequence as well (in the limit of $T_E = 0$). It is typical (but not necessary) that T_1 and T_2 correlate with spin density, i.e., a tissue with higher spin density usually has longer T_1 and T_2 values, and tissues with lower spin density usually have shorter T_1 and T_2 values. As a result, while T_1-weighting depicts tissues with longer T_1 values with low signal and short- T_1 tissues with higher signal, the spin density contrast counteracts this effect. Hence, a unique choice of T_R which maximizes the T_1-weighted contrast should exist. To optimize the T_1-weighted contrast, Equation B6.3.13 is extremized with respect to T_R. Differentiating C_{AB} with respect to T_R and setting it equal to zero leads to the relation:

$$\frac{\rho_{0,A} e^{-T_R/T_{1,A}}}{T_{1,A}} = \frac{\rho_{0,B} e^{-T_R/T_{1,B}}}{T_{1,B}} \qquad \textbf{(B6.3.14)}$$

Clearly, T_1-weighted imaging still has a strong dependence on spin density as well. Solving for T_R from Equation B6.3.14 gives the optimal T_R:

$$T_{R_{opt}} = \frac{\ln\left(\frac{\rho_{0,B}}{T_{1,B}}\right) - \ln\left(\frac{\rho_{0,A}}{T_{1,A}}\right)}{\left(\frac{1}{T_{1,B}} - \frac{1}{T_{1,A}}\right)} \qquad \textbf{(B6.3.15)}$$

Some a priori knowledge of tissue properties is clearly very useful. However, when several tissues are present, it may be difficult to choose a single T_R which optimizes all contrast and two scans with two different T_R values would be required.

This optimal value of T_R can also be obtained graphically by plotting the expression for C_{AB} from Equation B6.3.13 as a function of T_R. The optimal T_R value for gray matter (GM) and white matter (WM) can be shown to be 410 msec at 1.5 T (based on the parameters given in *UNIT B5.1*). Consider one such plot shown in Fig. B6.3.4A. At long T_R values, all tissues will have relaxed completely, and only spin density contrast is obtained, i.e., the contrast curve approaches a constant value asymptotically. At low values of T_R such that $T_R << T_1$ (this defines the T_1-weighted contrast regime), where the signal is inversely proportional to T_1, the tissue with shorter T_1 has a higher signal. In the case of gray matter and white matter, since white matter has the shorter T_1, it has a higher signal at short T_R values. However, since white matter also has a smaller spin density than gray matter, once T_R becomes comparable to T_1, gray matter starts growing towards a higher value, crossing the white matter curve towards its higher spin density value. The cross-over point represents the "null point" between gray matter and white matter where there is no contrast. For example, the null point where gray matter (spin density 0.8, T_1 = 950

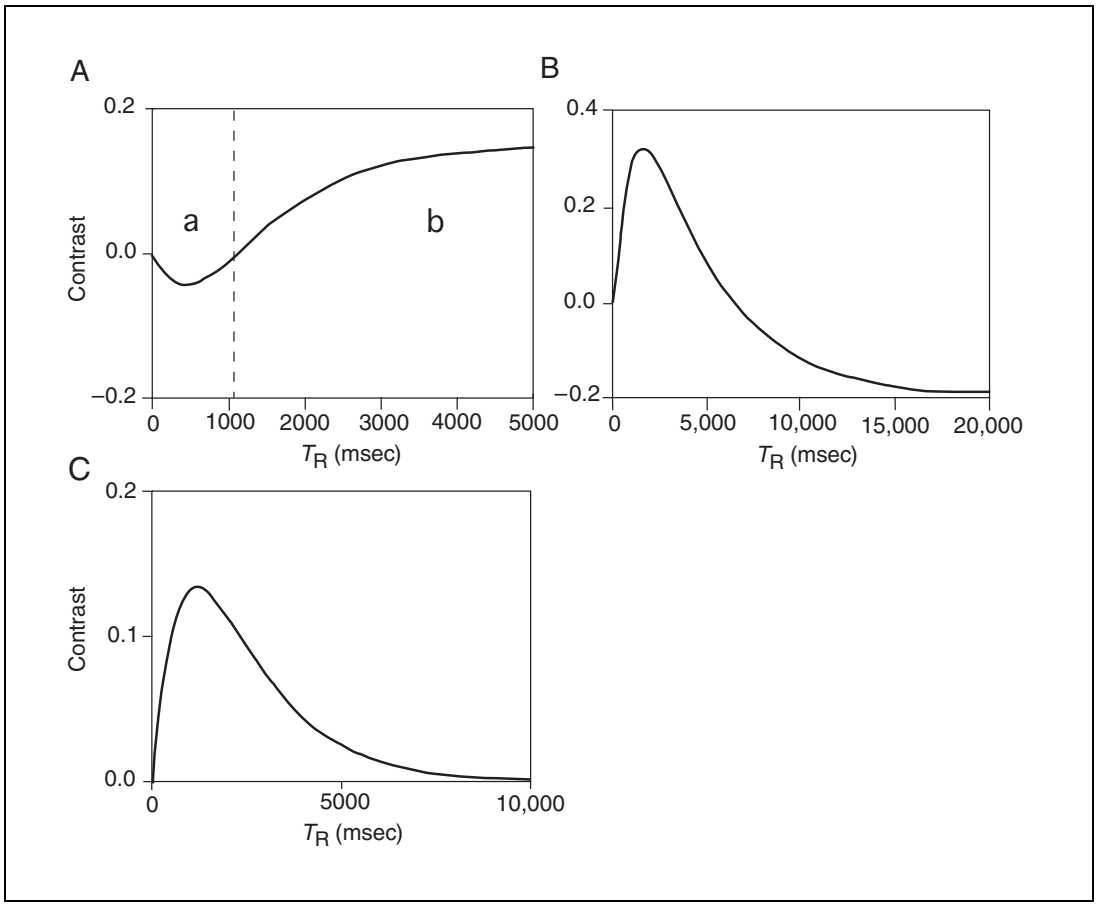

Figure B6.3.4 C_{AB} as a function of T_R for (**A**) GM/WM; (**B**) GM/CSF; (**C**) GM/lesion, in the case of a T_1-weighted 2-D or 3-D imaging experiment assuming ideal RF pulses. As demarcated in panel A, two regions can be identified for each plot: one where the contrast is T_1 weighted (e.g., region a in panel A), and another where the contrast is spin density-weighted (e.g., region b in panel A for example). The figure shows that a unique T_R value which optimizes either contrast can be identified for each tissue pair of interest (which varies according to the intended application). The lesion parameters were chosen to be $\rho_0 = 0.8$ and $T_1 = 1.5$ sec.

msec at 1.5 T) and white matter (spin density 0.65, $T_1 = 600$ msec at 1.5T) are iso-intense (i.e., they have the same signal) occurs at $T_R = 1050$ msec. In-between a T_R value of zero, where the contrast is zero, and the null point, there must be a maximum, and this represents the T_R value which gives the optimal T_1-weighted gray matter–white matter contrast. Two other examples, GM/CSF (cerebrospinal fluid; Fig. B6.3.4B) and GM/lesion ($\rho_0 = 0.8$, $T_1 = 1.5$ sec; Fig. B6.3.4C) are also shown for comparison. A "lesion" is used here to indicate abnormal tissue which contains T_1 and T_2 values larger than those of normal gray matter. Again, the previous observations are obeyed in both cases, and the range of T_R choices for the spin density weighting or T_1-weighting regimes can be determined from these plots.

Optimal T_R for tissues with similar spin densities and fractionally different T_1

The optimal value for T_R obtained in Equation B6.3.15 represents the most general case of two tissues A and B which have different spin densities. In the early stages of the formation of certain disease states, it is not uncommon to find the diseased tissue with a spin density which is very comparable to its normal neighbor, i.e.:

$$\rho_{0,A} \simeq \rho_{0,B} \equiv \rho_0 \quad \textbf{(B6.3.16)}$$

and a T_1 which is fractionally different. That is:

$$T_{1,B} = T_{1,A}(1+\delta) \quad \text{with } \delta \to 0 \quad \textbf{(B6.3.17)}$$

The expression for the contrast is:

$$\begin{aligned} C_{AB} &\simeq -\rho_0\left(e^{-T_R/T_{1,A}} - e^{-T_R/\left((1+\delta)T_{1,A}\right)}\right) \\ &\simeq \rho_0 e^{-T_R/T_{1,A}}\left(e^{\delta T_R/T_{1,A}} - 1\right) \\ &\simeq \rho_0 e^{-T_R/T_{1,A}}\left(\frac{T_R}{T_{1,A}}\right)\cdot\delta \end{aligned} \quad \textbf{(B6.3.18)}$$

where we used $e^{-T_R/((1+\delta)T_{1,A})} \cong e^{-(1-\delta)T_R/T_{1,A}}$. Maximizing with respect to T_R then yields:

$$T_{R_{opt}} = T_{1,A} \quad \textbf{(B6.3.19)}$$

i.e., for two tissues with comparable spin density and slightly different T_1 values, the optimal T_R to choose is the T_1 value of the shorter T_1 tissue.

Another commonly used mechanism for generating T_1 contrast is to use an inversion recovery sequence. The inversion recovery process offers the ability to null signal from a specific tissue by an appropriate choice of T_I (Inversion Time (T_I) = T_1ln2 in the limit $T_R >> T_1$). For example, the CSF signal or fat signal can be nulled by choosing a T_I value of 2.8 sec or 173.3 msec, respectively.

T_2- and T_2^*-weighting

The third basic contrast-generating mechanism is based on differences in the transverse decay characteristics. Most disease states are characterized by an elevated T_2. Since the T_2 values are only on the order of tens of milliseconds whereas T_1 values are typically on the order of a second, a small increase in T_2 corresponds to a larger percentage increase than the same increase in T_1. As a result, T_2 is found to be a sensitive indicator of disease. T_2-weighting can be obtained by using spin echo sequences. T_2^*-weighting also plays a useful role when local magnetic field susceptibility differences between tissues are present. If field changes occur sufficiently rapidly across a voxel, additional signal loss will occur when gradient echo sequences are used. For this reason, T_2^*-weighted images are used to study brain activity in brain functional imaging studies.

To avoid contributions from T_1 confounding the contrast, T_R is chosen such that:

$$T_R \gg T_{1_{A,B}} \Rightarrow e^{-T_R/T_1} \to 0 \quad \textbf{(B6.3.20)}$$

in which case the gradient echo contrast is given by:

$$C_{AB} = \rho_{0,A} e^{-T_E/T_{2,A}^*} - \rho_{0,B} e^{-T_E/T_{2,B}^*} \quad \textbf{(B6.3.21)}$$

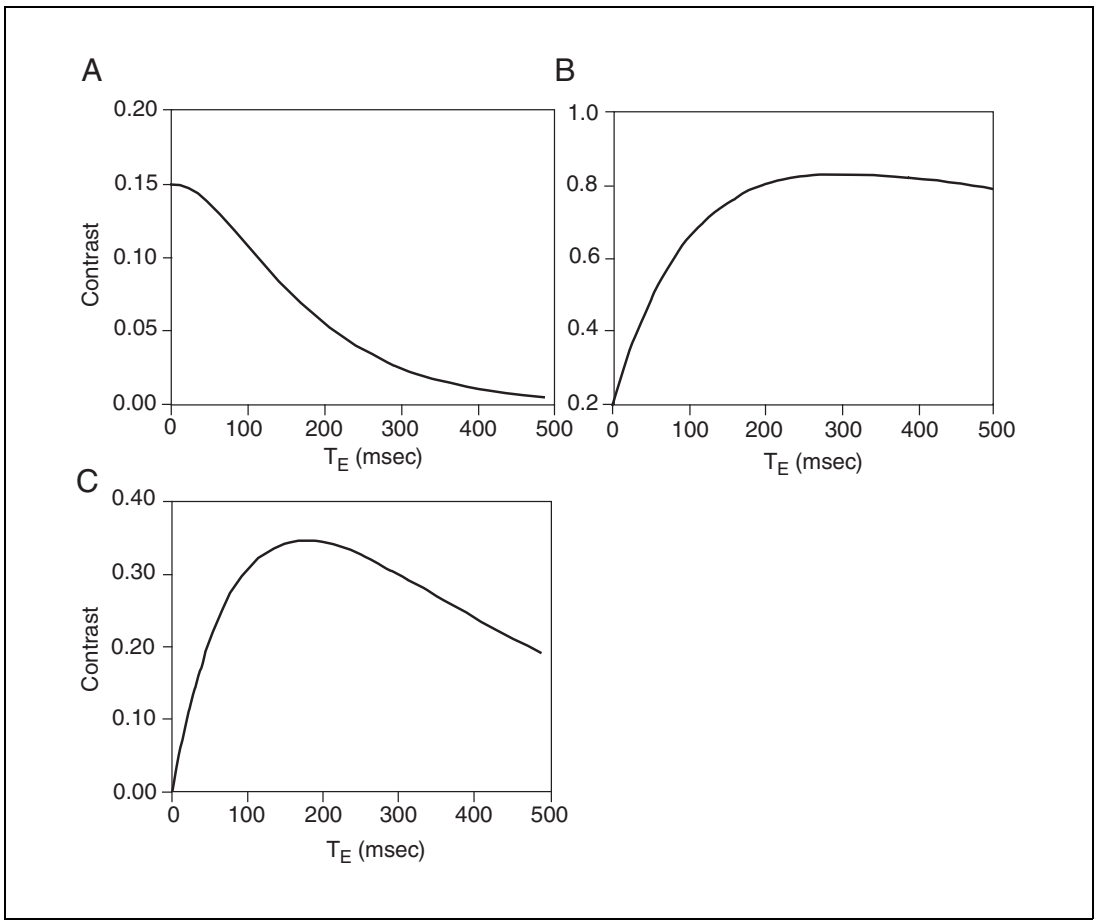

Figure B6.3.5 C_{AB} as a function of T_E for (**A**) GM/WM; (**B**) CSF/GM; and (**C**) lesion/GM for a T_2-weighted scan. C_{AB} is given in units relative to a maximal value of unity. An optimal T_E value can also be obtained for each pair of tissues from such plots.

Figure B6.3.5B shows a plot of T_E versus contrast for Equation B6.3.21 using gray matter ($\rho_0 = 0.8$ and $T_2 = 0.1$ sec) and CSF ($\rho_0 = 1.0$ and $T_2 = 2$ sec) as tissues *A* and *B*. Since GM has a T_2 value which is much shorter than that of CSF, the optimal T_E value is expected to be long compared to the T_2 value of gray matter and short compared to the T_2 value of CSF. On the other hand, when gray- and white-matter signals are considered as functions of T_E at long T_R values (Fig. B6.3.5A), WM ($\rho_0 = 0.65$ and $T_2 = 0.08$ sec) always has a signal that is lower than that of GM. So, the optimal GM-WM contrast is produced by a very short T_E, in the spin density-weighted regime. A similar contrast curve can be generated for any two tissues of interest, whose relative spin density and T_2 values are known. For example, the case of GM/lesion contrast is considered in Figure B6.3.5C. The lesion is assumed to have a ρ_0 of 0.8 and a T_2 of 350 msec. Since the contrast expression (Equation B6.3.21) contains only T_E dependence, optimal contrast is obtained by extremizing C_{AB} relative to T_E. The T_E at which the contrast is optimized is:

$$T_{E_{opt}} = \frac{\ln\left(\frac{\rho_{0,B}}{T^*_{2,B}}\right) - \ln\left(\frac{\rho_{0,A}}{T^*_{2,A}}\right)}{\left(\frac{1}{T^*_{2,B}} - \frac{1}{T^*_{2,A}}\right)} \qquad \textbf{(B6.3.22)}$$

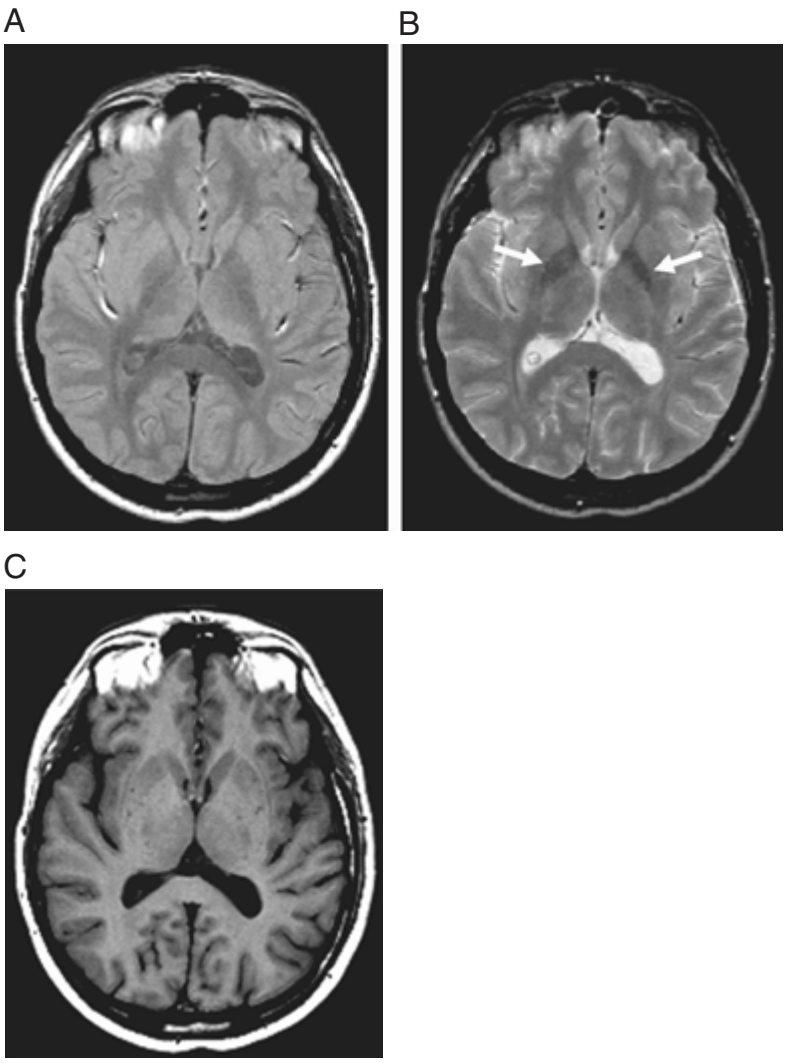

Figure B6.3.6 Different forms of contrast generated by varying the imaging parameters with a spin echo sequence. (**A**) Spin density-weighted image. (**B**) T_2-weighted image. (**C**) T_1-weighted image. Although (A) is supposed to indicate spin density, it fails to do so for CSF since T_1 of CSF is too long (4.5 sec) relative to the T_R (2.5 sec). Gray/white matter contrast is good. In (B), the globus pallidus (arrows) appears quite dark since the iron in it causes a diffusion-weighted signal loss. As expected, CSF is bright because of its long T_2 (2 sec). Lastly, in (C), gray/white matter contrast is reversed and CSF is heavily suppressed. The dark CSF regions seem to visually enhance the overall contrast in the image. The imaging parameters used were (A) T_R/T_E = 2500 msec/20 msec, $\theta = 90°$, T_s = 5.12 msec, $N_{acq} = 1$, $\Delta x \times \Delta y \times \Delta z$ = 1.0 mm × 1.0 mm × 5.0 mm, $N_x \times N_y = 256 \times 192$, τ_{RF} = 2.56 msec, G_{ss} = 2.4 mT/m; (B) T_E = 80 msec, T_s = 10.24 msec; (C) T_R = 650 msec, T_E = 14 msec, $\theta = 65°$, T_s= 11.2 msec, $N_{acq} = 2$.

As previously discussed, a similar expression is obtained for a spin echo experiment in terms of T_E with T_2^* replaced by T_2. Expressions for the optimal T_E in the special case of only a fractional difference in T_2 also gives results identical in form to the T_R choice for optimal T_1-weighted contrast—i.e., a T_E approximately equal to $T_{2,A}^*$ should be chosen.

Let us consider a physiologically relevant case. Suppose that the relative spin density (ρ_0), T_1, and T_2 values of a certain tissue (gray matter, say) are 0.8, 1 sec, and 100 msec, respectively. When disease sets in, suppose the local water content increases from 0% to 10% in each voxel. This two-compartment model implies that the fractional volume content of water in a voxel increases from 0 to 0.1 and that of the tissue decreases from 1.0 to 0.9. (The displaced tissue is simply pushed into an adjacent voxel.) If the T_1 and T_2 of water are 4 sec and 2 sec, respectively, then the signal measured from the voxel is essentially the sum of the healthy tissue and water signal weighted by their volume fractions. For a T_1-weighted scan (e.g., T_R = 20 msec, $\theta = 30°$, and $T_E = 0$), we see only 6.5% signal reduction in the diseased tissue when compared to healthy tissue. On the other hand, for a T_2-weighted scan (e.g., T_E = 100 msec, $\theta = 90°$, and infinite T_R), we see ~22.5% signal reduction in the diseased tissue when compared to healthy tissue. Therefore, T_2-weighted scan is much more sensitive to small changes in local water content.

The conclusion from the above case is that T_2-weighting might be the intrinsic contrast mechanism of choice for distinguishing diseased states from normal tissue. In fact, it therefore comes as no surprise that T_2-weighted spin echo sequences are used for a variety of clinical applications.

Summary of Contrast Results

The general appearance of spin density, T_1- and T_2-weighted images of the brain is depicted in the images shown in Figure B6.3.6. An optimal and yet practical set of imaging parameters was used to obtain these images. Clearly, the T_1-weighted imaging method seems to be the most efficient in achieving the contrast required. An intermediate T_R value of ~410 msec gives optimal GM-WM contrast and shows good differentiation between these two structures and CSF and fat. Fat, with the lowest T_1 value among these four tissues, is shown as the brightest structure. On the other hand, CSF is shown with almost no noticeable signal because of its long T_1. White matter is shown as the bright structure in the brain, while gray matter is shown with a lower gray level, all consistent with T_1-weighting. On the other hand, when it comes to spin density or T_2-weighting, it is impractical to design the sequence with a T_R which is on the order of a few T_1s of CSF. Therefore, it is typical to choose a T_R of about twice the T_1 of gray matter. At this T_R, CSF is almost iso-intense with white matter, and gray matter is found to have the highest signal. As described here, the spin density and T_2-weighted images shown in Figs. B6.3.6A and B6.3.6B were obtained using a T_R of 2.5 sec. On the T_2-weighted image, typically obtained using a longer T_E at the same T_R as the spin density-weighted image, CSF has the highest signal while white matter has the lowest signal. A set of general rules for choosing T_E and T_R for a $\pi/2$ gradient echo (or spin echo) experiment are outlined in Table B6.3.1.

LITERATURE CITED

Rose, A. 1985. Vision: Human and Electronic. Plenum Press, New York.

KEY REFERENCES

Constable, R.T. and Henkelman, R.M. 1991. Contrast, resolution, and detectability in MR imaging. *J. Comput. Assist. Tomogr.* 15:297.

The contrast and visibility in MR images are well described in this paper.

Haacke, E.M., Brown, R.W., Thompson, M.R., and Venkatesan, R. 1999. Magnetic Resonance Imaging: Physical Principles and Sequence Design. John-Wiley & Sons, New York.

The inherent contrast mechanisms along with contrast-to-noise ratio is well described in this text.

Venkatesan, R. and Haacke, E.M. 1997. Role of high resolution in magnetic resonance (MR) imaging: Applications to MR angiography, intracranial T_1-weighted imaging, and image interpolation. *Int. J. Imaging Sys. Technol.* 8:529.

The contrast and visibility in MR images are well described in this paper.

Contributed by Azim Celik
General Electric Company
Milwaukee, Wisconsin

Weili Lin
The University of North Carolina at Chapel Hill
Chapel Hill, North Carolina